Article

# Dehydrative Cyclocondensation Reactions on Hydrogen-Terminated Si(100) and Si(111): An ex Situ Tool for the Modification of Semiconductor Surfaces

Timothy R. Leftwich, Mark R. Madachik, and Andrew V. Teplyakov

*J. Am. Chem. Soc.*, **2008**, 130 (48), 16216-16223 • DOI: 10.1021/ja802645t • Publication Date (Web): 07 November 2008



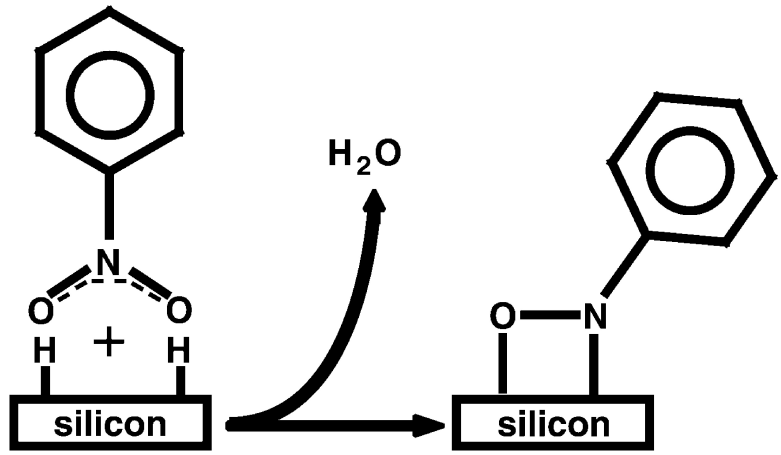


## More About This Article

Additional resources and features associated with this article are available within the HTML version:

- Supporting Information
- Access to high resolution figures
- Links to articles and content related to this article
- Copyright permission to reproduce figures and/or text from this article

View the Full Text HTML

J|A|C|S
ARTICLES

Published on Web 11/07/2008

# Dehydrative Cyclocondensation Reactions on Hydrogen-Terminated Si(100) and Si(111): An ex Situ Tool for the Modification of Semiconductor Surfaces

Timothy R. Leftwich, Mark R. Madachik, and Andrew V. Teplyakov*

*Department of Chemistry and Biochemistry, University of Delaware, Newark, Delaware 19716*

Received April 10, 2008; E-mail: andrewt@udel.edu

***Abstract:*** Dehydrative cyclocondensation processes for semiconductor surface modification can be generally suggested on the basis of well-known condensation schemes; however, in practice this approach for organic functionalization of semiconductors has never been investigated. Here we report the modification of hydrogen-terminated silicon surfaces by cyclocondensation. The cyclocondensation reactions of nitrobenzene with hydrogen-terminated Si(100) and Si(111) surfaces are investigated and paralleled with selected cycloaddition reactions of nitro- and nitrosobenzene with Si(100)-2×1. Infrared spectroscopy is used to confirm the reactions and verify an intact phenyl ring and C−N bond in the reaction products as well as the depletion of surface hydrogen. High resolution N *1s* X-ray photoelectron spectroscopy (XPS) suggests that the major product for both cyclocondensation reactions investigated is a nitrosobenzene adduct that can only be formed following water elimination. Both IR and XPS are augmented by density functional theory (DFT) calculations that are also used to investigate the feasibility of several surface reaction pathways, which are insightful in understanding the relative distribution of products found experimentally. This novel surface modification approach will be generally applicable for semiconductor functionalization in a highly selective and easily controlled manner.

## I. Introduction

Advancing microelectronics toward the use of molecular-size features requires a detailed and selective molecular-level control of the attachment chemistry. The molecular features produced by approaches similar to those of traditional homogeneous chemistry methods must be robust, stable in a variety of conditions, and reasonably easy to produce. Recently developed analogs of 1,3-dipolar cycloaddition, Diels−Alder reactions, and Grignard-type chemistry on Si(100)-2×1[1−7] together with temperature-dependent or photoinitiated chemistry of hydrogen-precovered silicon surfaces[8] brought about significant understanding of the parallels between semiconductor surface chemistry and methodological development of synthetic methods. The structural unit of the Si(100)-2×1 surface, a silicon−silicon dimer, has allowed the development of surface chemistry analogs of the reactions originally designed for unsaturated hydrocarbons and silenes. However, one of the most common reactions in organic and biochemistry, the reaction of dehydrative condensation, with the surface providing hydrogen for water formation, has not been explored on semiconductors. In fact, it is exactly since the byproduct of this reaction is water, the very molecule that should be avoided in silicon surface modification processes, that this chemistry has not been previously used on Si(100) or Si(111) surfaces. Of course, general condensation approaches are commonly used in such processes as atomic layer deposition (ALD), where surface hydroxyl groups are used as a source of hydrogen to ultimately form solid inorganic films.[9−12] However, because hydrogen-terminated single crystalline silicon surfaces are much easier to prepare and control, they can be used in a much broader array of current and potential applications as a starting point. A seeming disadvantage of using these surfaces is their chemical stability. Even when hydrogen-terminated silicon surfaces are used in ALD processes to form inorganic films,[11,13−16] oxygen incorporation from gas-phase impurities[17,18] and reactions with Si-OH sites[12] seem to dominate surface transformations.[12,17,18] For the reactions

(1) Wolkow, R. A. *Annu. Rev. Phys. Chem.* **1999**, *50*, 413–441.
(2) Wayner, D. D. M.; Wolkow, R. A. *J. Chem. Soc., Perkin Trans. 2* **2002**, 23–34.
(3) Bent, S. F. *Surf. Sci.* **2002**, *500*, 879–903.
(4) Barriocanal, J. A.; Doren, D. J. *J. Vac. Sci. Technol., A* **2000**, *18*, 1959–1964.
(5) Bocharov, S.; Teplyakov, A. V. *Surf. Sci.* **2004**, *573*, 403–412.
(6) Méndez De Leo, L. P.; Teplyakov, A. V. *J. Phys. Chem. B* **2006**, *110*, 6899–6905.
(7) Leftwich, T. R.; Teplyakov, A. V. *Surf. Sci. Rep.* **2008**, *63*, 1–71.
(8) Buriak, J. M. *Chem. Rev.* **2002**, *102*, 1271–1308.
(9) Halls, M. D.; Raghavachari, K. *J. Phys. Chem. B* **2004**, *108*, 4058–4062.
(10) Ghosh, M. K.; Choi, C. H. *Chem. Phys. Lett.* **2006**, *426*, 365–369.
(11) Rodriguez-Reyes, J. C. R.; Teplyakov, A. V. *Chem. Eur. J.* **2007**, *13*, 9164–9176.
(12) Kelly, M. J.; Han, J. H.; Musgrave, C. B.; Parsons, G. N. *Chem. Mater.* **2005**, *17*, 5305–5314.
(13) Ho, M. T.; Wang, Y.; Brewer, R. T.; Wielunski, L. S.; Chabal, Y. J.; Moumen, N.; Boleslawski, M. *Appl. Phys. Lett.* **2005**, *87*, 133103.
(14) Fenno, R. D.; Halls, M. D.; Raghavachari, K. *J. Phys. Chem. B* **2005**, *109*, 4969–4976.
(15) Halls, M. D.; Raghavachari, K. *J. Phys. Chem. A* **2004**, *108*, 2982–2987.
(16) Frank, M. M.; Chabal, Y. J.; Wilk, G. D. *Appl. Phys. Lett.* **2003**, *82*, 4758–4760.
(17) Halls, M. D.; Raghavachari, K.; Frank, M. M.; Chabal, Y. J. *Phys. Rev. B* **2003**, *68*.
(18) Halls, M. D.; Raghavachari, K. *J. Chem. Phys.* **2003**, *118*, 10221–10226.


**10.1021/ja802645t CCC: $40.75** 

discussed in this work, the surface is the only source of hydrogen, while the incoming molecule is the only source of oxygen for the formation of the cyclocondensation byproduct, water, which makes the reaction mechanism substantially easier to discern.

Ideal hydrogen-terminated silicon single crystal surfaces are generally considered rather unreactive and most chemical modifications for practical functionalization of these surfaces are initiated at surface defects. The vast majority of these functionalization schemes are dependent on radical initiation steps. Radical initiation can be achieved chemically, with the use of radical initiators,[19] photochemically,[20] electrochemically,[21] or thermally.[22] It should be noted that none of these reactions can allow for a reliable control of the surface coverage, if for example one would want to stop the reaction near a predetermined partial coverage. Unlike many of the reactions preformed with hydrogen-terminated silicon, cyclocondensation is not a radically initiated reaction. Of course, there are other reactions initiated using alternative compounds, such as, for example, with Lewis acids,[23] Karstedt (Pt-based) catalysts,[24] Grignard reagents ($CH_3(CH_2)_nMgX$, X = Br or Cl),[23] or alkyl lithium (with halogenated silicon).[25] Some of these do allow a degree of control over the surface reactions, but all of these processing schemes involve exposure of semiconductors to solutions that pose the danger of surface contamination.

The ultimate control over a radical-initiated reaction on a hydrogen-terminated silicon surface can only be achieved by using the truly ideal conditions of ultrahigh vacuum (UHV), where specific amounts of compounds can be dosed on the surface to produce a low coverage (for example, a line along the dimer rows of silicon on the hydrogen-terminated Si(100) surface),[26] or a "blocker" compound, such as 2,2,6,6-tetramethyl-1-piperidinyloxy (TEMPO),[27] can be used to stop the reaction. These reactions require a radical surface site (either initially present or produced artificially) and are difficult to perform in a controllable manner ex situ.

Here we report a simple, highly selective, and easily controllable thermal chemistry that is based on a cyclocondensation process, where hydrogen-terminated silicon substrates provide the source of hydrogen atoms and the incoming nitro-functionalized aromatic molecules provide an oxygen atom to form water. Since the miniscule amount of water produced corresponds to the monolayer coverage of hydrogen on the semiconductor substrate, this byproduct does not pose any contamination threat in nonaqueous conditions. This modification can be easily performed using standard equipment; it does not require any reaction initiators, photochemical steps, or the use of solutions of the modifier compound; and the rate (and thus surface coverage) can be fully controlled by thermal conditions. Such an approach can be generalized for surface functionalization of other semiconductors and with other participating reagents.

## II. Experimental Details

There are three types of surfaces used in these experiments. The first is clean Si(100)-2×1, which is prepared in ultrahigh vacuum (UHV) conditions in situ and is used as a reference. The other two are hydrogen-terminated Si(100) and hydrogen-terminated Si(111), which are prepared ex situ. After in situ chemical modification, the clean Si(100)-2×1 surface is either probed by infrared spectroscopy or removed from the ultrahigh-vacuum (UHV) chamber through the ambient environment to another UHV chamber for X-ray photoelectron spectroscopy (XPS) measurements.

The hydrogen-terminated silicon samples were prepared using a modified RCA[28] cleaning method followed by one of two oxide etching procedures. One procedure is used for the Si(100) wafers (Wafer World, Inc.) and another is used for the Si(111) wafers (Wafer World, Inc.). The Si(100) and the Si(111) wafers are polished on both sides. The RCA cleaning method used consists of three steps. The first step is the organic cleaning step using a (SC1) solution of a 4:1:1 ratio of Milli-Q water (Millipore) with a resistivity ≥18 MΩ·cm, hydrogen peroxide (30% certified ACS grade, Fisher Scientific), and ammonium hydroxide (29% certified ACS plus grade, Fisher Scientific), respectively, that is prepared in a Teflon beaker and placed in an 80 °C water bath for 10 min. Nitrogen was bubbled through an earlier batch of this same solution for 1 h to clean the Teflon beakers prior to use. The second step is an oxide etch using a buffered hydrofluoric acid solution (buffer-HF improved from Transene) for 2 min. The final step in this RCA method is an ionic cleaning step using a (SC2) solution of a 4:1:1 ratio of Milli-Q water (Millipore), hydrogen peroxide (30% certified ACS grade, Fisher Scientific), and hydrochloric acid (37.3% certified ACS grade, Fisher Scientific), respectively, prepared in a Teflon beaker and placed in an 80 °C water bath for 10 min. Vigorous rinsing with Milli-Q water (Millipore) is done after each of these steps. After the RCA cleaning, the silicon oxide surface is etched away leaving a hydrogen-terminated surface. Si(100) wafers are etched for 1 min in 48% hydrofluoric acid (J. T. Baker inc); Si(111) wafers are etched for 1 min in buffered hydrofluoric acid solution and then and additional 6 min with 40% ammonium fluoride solution (Fluka). The hydrogen-terminated Si(100) surface prepared by this procedure contains predominantly monohydride and dihydride surface sites, while the hydrogen-terminated Si(111) surface is covered predominantly with monohydride surface sites, as characterized by infrared spectroscopy measurements presented in section IV below. Chemical modification of these surfaces was done by refluxing nitrobenzene (99%, Sigma Aldrich) under nitrogen at 200 °C for 2 h. Modification of these surfaces with nitrobenzene was also conducted at room temperature and at 46 °C for selected experiments, as will be indicated below. The room-temperature experiment with a hydrogen-terminated Si(100) surface was conducted with a contact time of 11.5 h. The room-temperature experiment with a hydrogen-terminated Si(111) surface had a contact time of 2 days. The experiment at 46 °C was conducted with a contact time of 1.5 h.

Clean Si(100)-2×1 surfaces were prepared in an ultrahigh-vacuum chamber with a base pressure of better than $1 \times 10^{-9}$ Torr located in the Department of Chemistry and Biochemistry at the University of Delaware. This chamber is equipped with an ion gun, an Auger electron spectrometer (AES), and a low-energy electron diffraction (LEED) setup and is coupled to an infrared spectrometer. A Nicolet Magna 560 spectrometer with a liquid-nitrogen-cooled MCT detector was used to collect infrared spectra in situ for clean and chemically modified Si(100)-2×1 surfaces. A Nicolet Magna

(19) Linford, M. R.; Chidsey, C. E. D. *J. Am. Chem. Soc.* **1993**, *115*, 12631–12632.
(20) Effenberger, F.; Gotz, G.; Bidlingmaier, B.; Wezstein, M. *Angew. Chem., Int. Ed* **1998**, *37*, 2462–2464.
(21) Hunger, R.; Jaegermann, W.; Merson, A.; Shapira, Y.; Pettenkofer, C.; Rappich, J. *J. Phys. Chem. B* **2006**, *110*, 15432–15441.
(22) Sung, M. M.; Kluth, G. J.; Yauw, O. W.; Maboudian, R. *Langmuir* **1997**, *13*, 6164–6168.
(23) Boukherroub, R.; Morin, S.; Bensebaa, F.; Wayner, D. D. M. *Langmuir* **1999**, *15*, 3831–3835.
(24) Zazzera, L. A.; Evans, J. F.; Deruelle, M.; Tirrell, M.; Kessel, C. R.; McKeown, P. *J. Electrochem. Soc.* **1997**, *144*, 2184–2189.
(25) Bansal, A.; Li, X. L.; Lauermann, I.; Lewis, N. S.; Yi, S. I.; Weinberg, W. H. *J. Am. Chem. Soc.* **1996**, *118*, 7225–7226.
(26) Kirczenow, G.; Piva, P. G.; Wolkow, R. A. *Phys. Rev. B* **2005**, *72*.
(27) Pitters, J. L.; Wolkow, R. A. *J. Am. Chem. Soc.* **2005**, *127*, 48–49.
(28) Higashi, G. S.; Chabal, Y. J.; Trucks, G. W.; Raghavachari, K. *Appl. Phys. Lett.* **1990**, *56*, 656–658.

860 spectrometer with a liquid-nitrogen-cooled MCT detector was used to collect infrared spectra ex situ on freshly prepared and chemically modified hydrogen-terminated Si(100) and Si(111) surfaces. Clean Si(100)-2×1 surfaces were prepared on 25 mm × 20 mm × 1 mm Si(100) trapezoidal samples with 45° beveled edges (Harrick Scientific) for multiple internal reflection Fourier transform infrared spectroscopic (MIR-FTIR) studies, by sputtering with 0.5 keV $Ar^+$ ions for 1 h at room temperature, followed by annealing to temperatures up to 1150 K for 15 min, using an e-beam heater (McAllister Technical Services). The cleanliness of the surface was confirmed by AES. The argon (Matheson, 99.999%) for surface cleaning was used without additional purification.

For in situ infrared measurements, 2048 scans were collected at a resolution of 4 $cm^{-1}$. A spectrum of the clean surface was obtained as a background before the compound of interest was dosed through a leak value into the UHV chamber and the infrared spectrum was collected. Ex situ infrared spectra were collected in a single transmission mode. Five hundred and twelve scans were collected at a resolution of 8 $cm^{-1}$ for each spectrum. In one set of experiments a hydrogen-terminated Si(100) surface was used as the background and a chemically modified hydrogen-terminated Si(100) surface was used as the foreground. In the second set of single transmission experiments, a Si(100) wafer after RCA cleaning was used as the background and either a hydrogen-terminated Si(100) surface or a chemically modified hydrogen-terminated Si(100) surface was used as foreground. Both sets of experiments were also conducted with Si(111) with the same procedure. The ex situ single transmission infrared spectra were collected at an incident angle of 60° from the sample normal.

X-ray photoelectron spectroscopic (XPS) measurements were preformed at the Surface Analysis Facility in the Chemistry and Biochemistry Department of the University of Delaware using a VG ESCALAB 220i-XL electron spectrometer (VG Scientific, U.K.) operated at a pressure in the $10^{-9}$ mbar range. The source produces monochromatic Al Kα X-rays (1486.7 eV) and is operated at 15 kV, 8.9 mA, 120 W, and a 400 $\mu$m nominal X-ray spot size. Spectra are collected with a dwell time of 100 ms per point with a pass energy of 100 eV for survey spectra and 20 eV for high resolution spectra. Samples were rinsed three times with dichloromethane (certified ACS grade, Fisher Scientific) and three times with methanol (HPLC grade, Fisher Scientific), alternating between the two solvents, followed by drying with a stream of nitrogen to remove any unreacted nitrobenzene before collecting XPS measurements.

Nitrobenzene (99%, Sigma Aldrich) was purified by several freeze−pump−thaw cycles before being introduced into the UHV chamber, where its purity was confirmed in situ by mass spectrometery (SRS 200 mass spectrometer). Nitrobenzene was bubbled with nitrogen prior to being syringe pumped into nitrogen-filled glassware when it was used to modify hydrogen-terminated Si(100) and Si(111) surfaces ex situ. Nitrosobenzene (98%, Fluka) was purified by several pumping cycles. It was heated to 50 °C prior to dosing, and its purity was confirmed in situ by mass spectrometry.

## III. Computational Methods

Theoretical predictions of vibrational frequencies and N *1s* binding energies were obtained using the B3LYP hybrid density functional[29,30] and the 6-311+G(d,p) basis set[31] in the Gaussian 03 suite of programs.[32] A silicon cluster representing a single surface dimer adsorption site, $Si_9H_{12}$, was used to model the Si(100)-2×1 surface. In this cluster, silicon atoms representing subsurface silicon are hydrogen-terminated to preserve silicon hybridization. This same cluster was used after adding two hydrogens, $Si_9H_{14}$, or four hydrogens, $Si_9H_{16}$, to the silicon dimer, and reoptimizing, to model the monohydride- and dihydride-terminated Si(100) sites, respectively. A $Si_{17}H_{24}$ cluster was used to model monohydride-terminated Si(111). Comparative calculations were preformed with and without constraining the positions of the atoms representing the third subsurface layer and beyond for selected structures on the Si(100) surface. The N *1s* binding energies and vibrational frequencies predicted by both approaches are in close agreement with one another. The results from the fixed subsurface calculations were used in preparing the figures for this manuscript. The calculations for the Si(111) surface were performed without restricting any atomic positions. The N *1s* binding energies are predicted based on a Koopman's theorem approach, from the Kohn−Sham eigenvalues corresponding to the nitrogen *1s* core level of the fully optimized structures. The absolute energies were calibrated by comparing the N *1s* core energies predicted computationally for paranitroaniline, also using the B3LYP functional with a 6-311+G(d,p) basis set, and the experimentally measured values.[33] A more detailed procedure and discussion of this calibration is a subject of a separate publication. Vibrational calculations were preformed on optimized structures and scaled by a factor of 0.9605 to minimize systematic errors. This factor was obtained by comparing the Si−H stretch for hydrogen-terminated Si(111) predicted with the cluster calculations and our experimental data, which are also consistent with the known literature value.[34]

## IV. Results and Discussion

Scheme 1 shows both a general condensation reaction (A) and the general cyclocondensation process for nitrobenzene with a hydrogen-terminated silicon surface (B). In the latter process, nitrobenzene reacts with the hydrogen-terminated silicon surface, removing surface hydrogen, to form water and a nitrosobenzene adduct. The same adduct could be formed by 1,2-cycloaddition of nitrosobenzene with a clean Si(100)-2×1, as also shown in Scheme 1 (C), and thus the well-defined *cycloaddition* product could serve as a model to investigate spectroscopic characteristics of the *cyclocondensation* product.

With this in mind, an infrared spectroscopy investigation was performed to confirm the cyclocondensation reaction. Infrared investigations confirmed the loss of hydrogen from the surface, as well as the presence of a molecular fragment with the C−N bond and the phenyl ring intact. This study is summarized in Figure 1. Spectrum 1 examines the reaction of nitrobenzene with a hydrogen-terminated Si(111) surface, and spectrum 2 examines the reaction of nitrobenzene with hydrogen-terminated Si(100). Both of these spectra use hydrogen-terminated silicon, cut in the same crystallographic direction, as background. As will be discussed later, the major product of the cyclocondensation process is a nitrosobenzene adduct, and thus a comparison with a multiple internal reflection FTIR spectrum of nitrosobenzene reacted with a clean Si(100)-2×1 surface under UHV conditions is presented in this figure as spectrum 3. Notably, the spectral region of 2000−2200 $cm^{-1}$ confirms the loss of surface hydrogen during the cyclocondensation process, as the negative absorption corresponding to the Si−H stretches is observed at 2084 $cm^{-1}$ for the reaction with the hydrogen-terminated Si(111), spectrum 1, and at approximately 2108 and 2084 $cm^{-1}$ for the major and minor components, respectively, of the reaction with hydrogen-terminated Si(100), spectrum 2. It should be noted the that this spectroscopic signature confirms that the hydrogen-

(29) Becke, A. D. *J. Chem. Phys.* **1993**, *98*, 1372–1377.
(30) Lee, C. T.; Yang, W. T.; Parr, R. G. *Phys. Rev. B* **1988**, *37*, 785–789.
(31) Krishnan, R.; Binkley, J. S.; Seeger, R.; Pople, J. A. *J. Chem. Phys.* **1980**, *72*, 650–654.
(32) Frisch, M. J.; et al. *Gaussian 03, Revision C.02*; Gaussian, Inc.: Wallingford, CT, 2004.
(33) Agren, H.; Roos, B. O.; Bagus, P. S.; Gelius, U.; Malmquist, P. A.; Svensson, S.; Maripuu, R.; Siegbahn, K. *J. Chem. Phys.* **1982**, *77*, 3893–3901.
(34) Zhang, X.; Garfunkel, E.; Chabal, Y. J.; Christman, S. B.; Chaban, E. E. *Appl. Phys. Lett.* **2001**, *79*, 4051–4053.

***Scheme 1.*** Schematic Representation of (A) Condensation Reaction; (B) Cyclocondensation Reaction of Nitrobenzene with Hydrogen-Terminated Silicon; (C) Cycloaddition Reaction of Nitrosobenzene with Si(100)-2×1

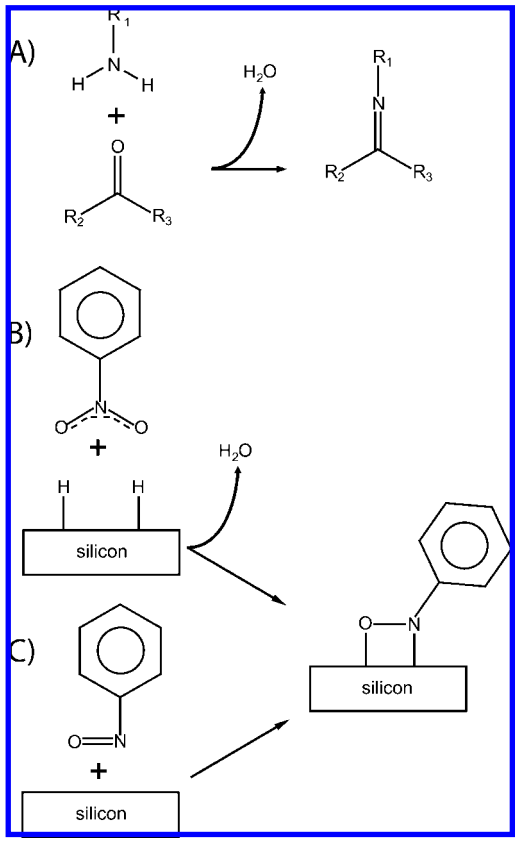


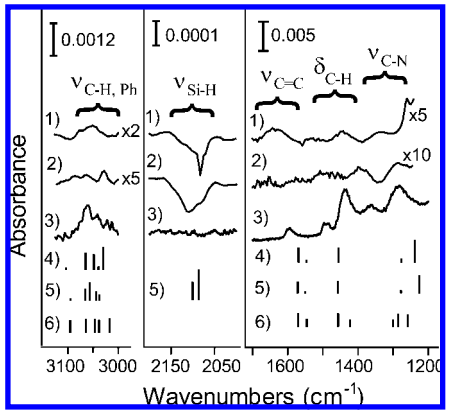


***Figure 1.*** Infrared investigation of cycloaddition and cyclocondensation processes on silicon. (1) Single transmission FTIR spectrum of nitrobenzene reacted with a hydrogen-terminated Si(111) surface (hydrogen-terminated Si(111) surface as a background). (2) Single transmission FTIR spectrum of nitrobenzene reacted with a hydrogen-terminated Si(100) surface (hydrogen-terminated Si(100) surface as a background). (3) MIR-FTIR spectrum of nitrosobenzene reacted with a clean Si(100)-2×1 surface in UHV (clean Si(100)-2×1 surface as a background). (4) Infrared spectrum predicted for the major nitrosobenzene adduct produced after a reaction of nitrobezene with hydrogen-terminated Si(111) and (5) with hydrogen-terminated Si(100). (6) Infrared spectrum predicted for the major nitrosobenzene adduct produced after a reaction of nitrosobezene with Si(100)-2×1. Three different spectral regions are presented because of significant intensity differences among them.

terminated Si(111) surface consists predominatly of monohydride surface species and that the hydrogen-terminated Si(100) surface consists predominantly of monohydride and dihydride

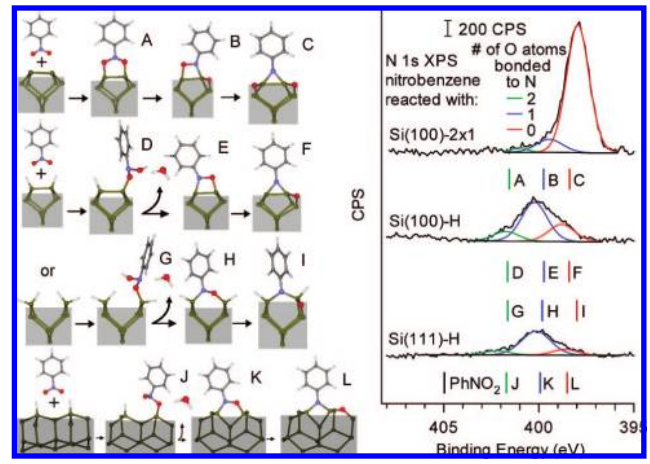


***Figure 2.*** Comparison of the 1,3-cycloaddition reaction of nitrobenzene with a Si(100)-2×1 surface with the condensation reactions of nitrobenzene with an ideal monohydride-terminated Si(100) surface, a dihydride-terminated Si(100) surface, and an ideal monohydride-terminated Si(111) surface, descending order on the left. The ex situ high resolution N *1s* XPS spectra, with the predicted N *1s* binding energy of the corresponding products, after these reactions occur, and nitrobenzene itself, are presented on the right of the respective reaction. Computations were preformed at the B3LYP/6-311+G(d,p) level of theory. Color coding: green, silicon; blue, nitrogen; gray, carbon; white, hydrogen. The same color coding is used in all other figures. The nitrobenzene reaction with the Si(100)-2×1 surface was performed in ultrahigh vacuum as described previously, and the XPS spectrum was collected ex situ. The condensation reaction was performed under nitrogen ex situ. On the schematic, hydrogen atoms terminating the silicon clusters are omitted for clarity.

surface species.[28,34−36] In addition to mono- and dihydride sites, hydrogen termination of Si(100) substrates etched with hydrofluoric acid solutions produces more complex structures,[34,37] including (111) terraces, which have been observed on this substrate.[38] Evidence for a small population of trihydide-terminated silicon can also be observed at approximately 2140 $cm^{-1}$ for the hydrogen-terminated Si(100).[34] Despite possible differences of the products of these reactions caused by nonuniformity of the hydrogen-terminated Si(100) substrate, the key vibrational features representing the phenyl ring and the C−N bond are clearly observed in both cases. These vibrational features are recorded even more clearly on the more uniform hydrogen-terminated Si(111) surface. The C−H stretches indicate that the phenyl ring remains intact after the reaction, since the only C−H modes in this region correspond to the aromatic compounds. To confirm the assignment, the predicted spectra for the initial major nitrosobenzene adducts formed after the reaction with hydrogen-terminated Si(111), hydrogen-terminated Si(100), and a clean Si(100)-2×1 surface, shown in Figure 2 as structures K, H, and E, are summarized in Figure 1 as spectra 4, 5, and 6, respectively. Since according to the experimental observation there are more dihydrogen bonded silicon sites than monohydrogen bonded silicon sites on hydrogen-terminated Si(100), the nitrosobenzene adduct formed from the reaction of nitrobenzene with a dihydride Si(100) site was used in spectrum 5. It should be noted that the nitrosobenzene adduct produced from a reaction with a dihydride species has silicon hydrogen bonds that are amenable to further cyclocondensation

(35) Chabal, Y. J.; Higashi, G. S.; Raghavachari, K.; Burrows, V. A. *J. Vac. Sci. Technol. A* **1989**, *7*, 2104–2109.
(36) Jakob, P.; Chabal, Y. J. *J. Chem. Phys.* **1991**, *95*, 2897–2909.
(37) Boland, J. J. *Adv. Phys.* **1993**, *42*, 129–171.
(38) Faggin, M. F.; Green, S. K.; Clark, I. T.; Queeney, K. T.; Hines, M. A. *J. Am. Chem. Soc.* **2006**, *128*, 11455–11462.

reactions. Less than 5% of all Si−H bonds are left on the surface after cyclocondensation (see Supporting Information for details). Finally, it can be noted that the reaction of nitrobenzene with a clean Si(100)-2×1 surface, studied in detail previously,[5,6] can also serve as a comparison with the cyclocondensation reaction; however, it yields a rather complex distribution of products with similar vibrational signatures and only a small population of the nitrosobenzene adduct.

So far, we have considered the nitrosobenzene adducts as the only products formed by the cyclocondensation process; however, further surface transformations can be caused by subsurface oxygen migration and lead to the formation of additional surface structures. Although IR can confirm the presence of a C−N bond and an intact phenyl ring, the exact identification of the final result of the cyclocondensation process is impractical with this spectroscopic technique, as many of the possible products have similar predicted vibrational spectra. As will be discussed in detail below, most of the differences among the possible final products of the cyclocondensation process manifest themselves in different chemical environments of the nitrogen atom. Fortunately, X-ray photoelectron spectroscopy (XPS) can distinguish similar products on this basis. Thus, the high resolution N *1s* XPS spectrum recorded following the cyclocondesation reaction should be the most informative XPS spectrum to examine.

The right side of Figure 2 shows the high resolution N *1s* XPS spectrum collected after the reaction of nitrobenzene with a Si(100)-2×1, hydrogen-terminated Si(100), and a hydrogen-terminated Si(111) surface. The left side of Figure 2 shows the reaction schemes for these reactions, with the products labeled A−L. The predicted N *1s* binding energies for structures A−L as well as for nitrobenzene itself are shown as bars at the bottom of corresponding XPS spectra in Figure 2. The specific N *1s*assignments are based on the previous studies of nitromethane,[39] which behaves similarly to nitrobenzene on a clean Si(100)-2×1 surface,[5,6] and the computational prediction of the core-level energies for the N *1s* region of the spectrum for all the models considered.

The reaction of nitrobenzene with a clean Si(100)-2×1 surface has been studied extensively[5,6] and has products that are similar to those produced by cyclocondensation. It proceeds via 1,3-cycloaddition, to form structure A, followed by subsurface oxygen migration, to form structures B and then C. Because it has products where there are not only one or zero oxygen atoms attached to nitrogen but also one with two oxygen atoms attached to nitrogen, the N *1s* XPS spectrum after the reaction of nitrobenzene with a clean Si(100)-2×1 surface is also shown in Figure 2 for comparison. While the cyclocondesation reaction can indeed form water and a nitrosobenzene adduct as products, it can also form a stable intermediate prior to water evolution and a product where the oxygen of the nitrosobenzene adduct migrates subsurface. These products are shown on the left side of Figure 2, starting with the stable intermediate, continuing with the nitrosobenzene adduct, and concluding with the product of oxygen migration subsurface, for the reaction of nitrobenzene with three different hydrogen-terminated silicon reactive sites. The first of these is a monohydride-teminated Si(100) site leading to the formation of products D−F. The second site considered is dihydride-terminated Si(100) with resulting products G−I. The final type of surface reactive site considered is monohydride-terminated Si(111) with resulting products J−L. Dihydride-terminated Si(100) is used to model the majority site on the hydrogen-terminated Si(100), while monohydride-terminated Si(100) and Si(111) are used to model the minority sites on this surface. The monohydride-terminated Si(111) site is also used to model the hydrogen-terminated Si(111) surface.

Structures B, C, F, I, and L are not the only possible structures for oxygen migration; however, they are the thermodynamically favored structures. Structures B and C were shown to be more thermodynamically stable than the structures produced by oxygen insertion into the Si−Si dimer bond.[6] Because of the similarity of structures F and I to structures B and C, these structures should also be more thermodynamically stable than the structures produced by oxygen insertion into the Si−Si dimer bond. Structure L is 97.6 kJ/mol more stable than the structure produced by oxygen insertion to produce a five-membered Si-N-Si-O-Si- ring.

Computational comparison of the N *1s* binding energies in species A, D, G, and J as opposed to B, E, H, and K or C, F, I, and L in Figure 2 confirms that while probing the species formed on this surface by nitrobenzene, this spectroscopic characteristic mostly depends on the number of oxygen atoms connected to nitrogen, rather than on a specific surface structure. Thus, based on the spectra presented in Figure 2 and our computational studies, the major products of these cyclocondensation reactions have a nitrogen atom that is bonded to only one oxygen atom. This along with the vibrational data presented in Figure 1, which shows that both the phenyl ring and C−N bond remain intact after the reaction, indicates that the major product of cyclocondensation is a nitrosobenzene adduct that could be of the type of structures E or H for hydrogen-terminated Si(100) and K for hydrogen-terminated Si(111). The approximate distribution of the products following the cyclocondensation process, on both hydrogen-terminated Si(100) and Si(111), is 25% for phenylnitrene adducts, 55% for nitrosobenzene adducts, and 20% for the rest of the possible adducts. In contrast, based both on previous studies[5,6] and the XPS data presented in Figure 2, the major product of the nitrobenzene cycloaddition reaction on a clean Si(100)-2×1 surface is a phenylnitrene adduct of the type of structure C, which constitutes over 80% of the product population.

Structures E, H, and K are the ones used for the vibrational frequency calculations presented in Figure 1 as spectra 6, 5, and 4, respectively. Structure E is used in Figure 1 spectrum 6, even though it is the expected product of cyclocondensation of nitrobenzene with monohydride Si(100), because it is also an expected product of 1,2-cycloaddition of nitrosobenzene with Si(100)-2×1.

It should be noted that if the nitro group were left intact after the reaction with the surface, then on the basis of the computational prediction, there would be a peak in the N *1s* XPS spectrum expected around 406 eV, close to the predicted core level energy for the nitrogen atom in nitrobenzene (as indicated by a black line at the bottom right of Figure 2 for $PhNO_2$); however, this is not the case. This peak is observed after the electrochemical reaction of the diazonium salt of nitrobenzene with hydrogen-terminated Si(111),[21] where the diazonium salt of nitrobenzene is believed to react through the phenyl ring and not the nitro group. Although the hetero-[4 + 2] reaction of nitrobenzene with the surface, which involves both the nitro group and a double bond in the phenyl ring, would not produce a peak around 406 eV in the high resolution N *1s* XPS spectra, it is not an expected product according to other

(39) Eng, J.; Hubner, I. A.; Barriocanal, J.; Opila, R. L.; Doren, D. J. *J. Appl. Phys.* **2004**, *95*, 1963–1968.

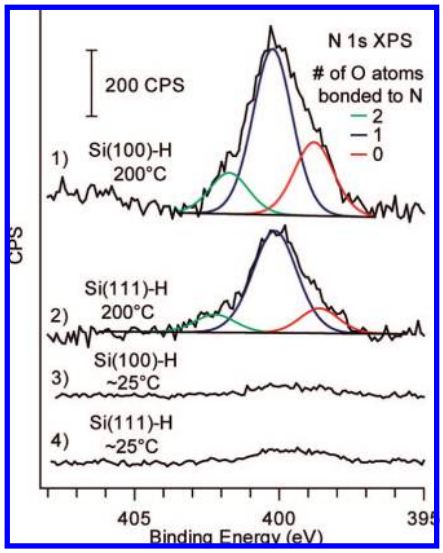


***Figure 3.*** Comparison of the ex situ high resolution N *1s* XPS spectra after the cyclocondensation reaction of nitrobenzene conducted at 200 °C for 2 h with (1) hydrogen-terminated Si(100) and (2) hydrogen-terminated Si(111) and the same reaction conducted at room temperature with (3) hydrogen-terminated Si(100) for 11.5 h and (4) hydrogen-terminated Si(111) for 2 days.

studies of nitrobenzene reacted with silicon surfaces[5,6] and is indeed not a major product in the cyclocondensation reaction as indicated by the presence of aromatic C−H stretches in the infrared spectra, Figure 1. Additionally, no evidence of Si−C bonds was observed in the C *1s* or Si *2p* high resolution XPS spectra (not shown) collected following cyclocondensation. The predicted binding energies for products A-L correlate well with the values observed in the XPS spectra and with a similar compound, nitromethane, previously studied on a clean Si(100)-2×1 surface.[39]

Some conclusions may also be inferred by comparing the relative peak areas of the N *1s* XPS spectra collected following the condensation reaction on hydrogen-terminated Si(100) and Si(111). Figure 2 suggests that the peak area of the N *1s* spectrum of hydrogen-terminated Si(100) following the condensation reaction is not only comparable to but is actually greater than that of the same reaction on hydrogen-terminated Si(111). Although there may be microfacets of hydrogen-terminated Si(111) on hydrogen-terminated Si(100), they are only a minor component of the surface. Therefore, since the N *1s* peak area is larger for the condensation reaction on hydrogen-terminated Si(100) compared to that of hydrogen-terminated Si(111), the reaction of nitrobenzene with the hydrogen-terminated Si(100) surface is not limited to hydrogen terminated Si(111) sites. The hydrogen-terminated Si(100) is predominately dihydride. The cyclocondensation reaction with dihydride sites results in the products that in turn also have Si−H bonds that are amenable to further cyclocondensation reactions. In addition it is likely that the hydrogen-terminated Si(100) surface has more defects than the H-terminated Si(111) surface.

Although all of the experimental data presented so far for the cyclocondensation process was obtained after reactions performed at 200 °C, room temperature reactions were also investigated. Figure 3 shows the high resolution N *1s* XPS spectra, previously shown in Figure 2, collected following the reaction of nitrobenzene at 200 °C for 2 h with hydrogen-terminated Si(100), spectrum 1, and hydrogen-terminated Si(111), spectrum 2, as well as the high resolution N *1s* XPS spectra after the room-temperature reaction of nitrobenzene with hydrogen-terminated Si(100) for 11.5 h, spectrum 3, and hydrogen-terminated Si(111) for 2 days, spectrum 4. The comparison of these spectra suggests that for both surfaces there is essentially a negligible amount of nitrogen on silicon substrates reacted at room temperature compared to the modification at 200 °C. The peak area obviously correlates with the surface coverage of the cyclocondensation products. This indicates that there is a substantial barrier for the cyclocondensation process and that thermal conditions can help provide an easy control over this reaction.

To fully utilize thermal control of this process, an estimate of the reaction barrier is needed. Fortunately, DFT calculations can predict this barrier. The full details of this computational investigation are explained in detail below; however, the barriers for the first step of the cyclocondensation reaction, which also happen to be the barriers for the overall cyclocondensation process, can be briefly recounted here. For hydrogen-terminated Si(111) this barrier is predicted, using a monohydride-terminated Si(111) cluster, to be 140.1 kJ/mol. Predicting the barrier for hydrogen-terminated Si(100) is slightly more complex. One must remember that hydrogen-terminated Si(100) is a mixture of monohydride- and dihydride-terminated silicon sites. Each of these sites must be examined individually to understand the properties of the entire surface. Monohydride-terminated Si(100) sites have a predicted barrier of 142.1 kJ/mol, while dihydride-terminated Si(100) sites have a predicted barrier of 160.4 kJ/mol. This suggests that the monohydride-terminated silicon sites, both Si(100) and Si(111), are more reactive than the dihydride-terminated Si(100) sites. This would in turn suggest that initially the reaction with hydrogen-terminated Si(100) should proceed preferentially via monohydride-terminated silicon sites and that the reaction barrier for the surface will increase after these sites react.

One may assume that this predicted reactivity difference between the monohydride- and dihydride-terminated silicon reactive sites can be observed experimentally with infrared spectroscopy if the cyclocondensation reaction of nitrobenzene with hydrogen-terminated Si(100) is interrupted before it is complete. Unfortunately, even though both monohydride- and dihydride-terminated silicon reactive sites are present on hydrogen-terminated Si(100), the predicted initial major product of the reaction of nitrobenzene with a dihydride-terminated silicon site, structure H, exhibits a Si−H stretch that is predicted to be in the same spectral region, around 2084 $cm^{-1}$, as monohydride-terminated silicon. Figure 4 shows the Si−H stretch region of the infrared spectra of hydrogen-terminated Si(100) before its reaction with nitrobenzene (spectrum 1), after a reaction with nitrobenzene at 46 °C for 1.5 h (spectrum 2) and after the reaction is run to completion at 200 °C (spectrum 3). The predicted infrared spectrum of structure H, the initial major product of the reaction of nitrobenzene with a dihydride-terminated silicon site is also shown in Figure 4, as spectrum 4. The experimental results summarized in Figure 4 confirm that the intensity of the $\upsilon_{Si-H}$ absorption bands corresponding to both monohydride- and dihydride-terminated silicon decreases essentially simultaneously and that there is still monohydride-terminated silicon present after the reaction is interrupted before completion. Thus, since the presence of monohydride-terminated silicon after the reaction can indicate either the lack of difference in reactivity between monohydride and dihydride surface sites or, on the contrary, efficient reaction of silicon monohydride with less efficient reaction of silicon dihydride leading to the

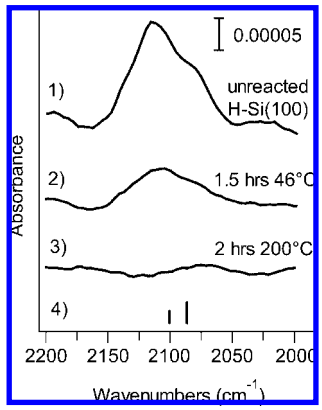


***Figure 4.*** (1) Infrared spectrum of the Si−H stretch region of a hydrogen-terminated Si(100) surface. (2) Infrared spectrum of the Si−H stretch region of a hydrogen-terminated Si(100) surface after a 1.5-h reaction with nitrobenzene at 46 °C. (3) Infrared spectrum of the Si−H stretch region of a hydrogen-terminated Si(100) surface after a 2-h reaction with nitrobenzene at 200 °C. (4) Predicted infrared spectrum of the Si−H stretch region of structure H.

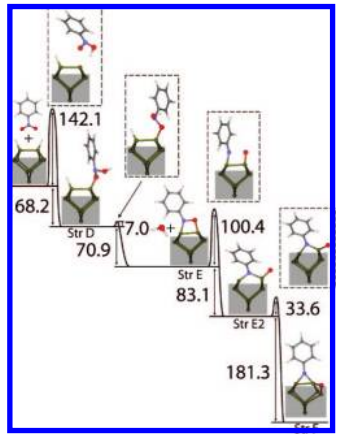


***Figure 5.*** Condensation reaction of nitrobenzene with a monhydride-terminated Si(100) surface represented by a $Si_9H_{14}$ cluster. Computations were performed at the B3LYP/6-311+G(d,p) level of theory. Hydrogen atoms representing silicon cluster termination are omitted for clarity. All energies are reported in kJ/mol and are not corrected for zero point vibrational energy.

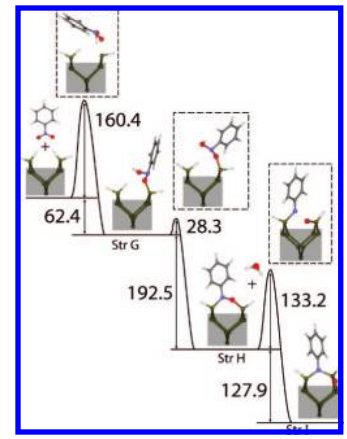


***Figure 6.*** Condensation reaction of nitrobenzene with a dihydride-terminated Si(100) surface represented by a $Si_9H_{16}$ cluster. Computations were performed at the B3LYP/6-311+G(d,p) level of theory. Hydrogen atoms representing silicon cluster termination are omitted for clarity. All energies are reported in kJ/mol and are not corrected for zero point vibrational energy.

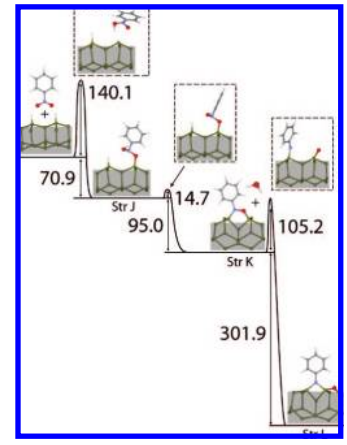


***Figure 7.*** Condensation reaction of nitrobenzene with a monohydride-terminated Si(111) surface represented by a $Si_{17}H_{24}$ cluster. Computations were performed at the B3LYP/6-311+G(d,p) level of theory. Hydrogen atoms representing silicon cluster termination are omitted for clarity. All energies are reported in kJ/mol and are not corrected for zero point vibrational energy.

formation of the structures of type H (also monohydride characterized by an insufficient difference of vibrational signatures compared to a clean hydrogen-terminated Si(100) surface), these experimental observations cannot point to an exclusive preference of one of these scenarios over the other.

DFT calculations can also be used to predict the barriers between the individual steps of the cyclocondensation process, which will help to understand the distribution of products observed in XPS experiments. Figures 5, 6, and 7 show the computationally predicted reaction diagrams for the cyclocondensation process of nitrobenzene with a monohydride-terminated Si(100), a dihydride-terminated S(100), and a monohydride-terminated Si(111) surface site, respectively.

The first observation obtained by examining the reaction diagrams for the cyclocondensation process is that after the initial barrier for the first step is overcome, the rest of the reaction steps proceed downhill compared to the energy of the hydrogen-terminated silicon surface and a nitrobenzene molecule. The second observation is that after the initial cyclocondensation product (nitrosobenzene adduct) is formed (structure E in Figure 5, structure H in Figure 6, and structure K in Figure 7), there is a substantial barrier required for the oxygen atom of these nitrosobenzene adducts to migrate into the silicon substrate. The 1,3-cycloaddition process of nitrobenzene with Si(100)- 2×1, shown in the top left of Figure 2, has been previously studied by our group, and the barrier for oxygen migration from the nitrosobenzene adduct in this process, when using a cluster with a fixed subsurface, is 82.6 kJ/mol.[6] The barriers for oxygen migration in Figures 5, 6, and 7 from nitrosobenzene adducts E, H, and K, respectively, are noticeably higher, explaining why these nitrosobenzene adducts are formed preferentially, as oxygen migration occurs easily after 1,3-cycloaddition of nitrobenzene to the clean Si(100)-2×1 surface. It can also be added that the desorption barriers for nitrosobenzene from these nitrosobenzene adducts are incomparably higher. The barrier to yield a gas phase nitrosobenzene and a clean surface from structure E is predicted to be 241.4 kJ/mol. The barrier to yield a gas phase nitrosobenzene and a clean surface from structure K is predicted to be 351.7 kJ/mol.

The difference in product distribution between the 1,2-cycloaddition of nitrosobenzene on Si(100)-2×1 and the condensation reaction of nitrobenzene on hydrogen-terminated

Si(100) can also be partially explained by the difference in the barriers for subsurface oxygen migration. Structure E in Figure 5 is the product of either the nitrobenzene cyclocondensation on hydrogen-terminated Si(100) surface or the [2 + 2] cycloaddition of nitrosobenzene with a clean Si(100)-2×1 surface. As such, the computational description of subsurface oxygen migration following the formation of structure E by either one of these processes is exactly the same. When the first barrier for oxygen migration, in Figure 5, is compared to the barrier for oxygen migration in the dihydride-terminated Si(100) diagram, Figure 6, it is found that the latter is 32.8 kJ/mol higher. Thus, the specific surface structure can also alter the distribution of the products in a cyclocondensation process. A more detailed examination of the 1,2-cycloaddition of nitrosobenzene with Si(100)-2×1 and its comparison to the cyclocondensation reaction of nitrobenzene with hydrogen-terminated silicon will be a subject of a separate publication.

There are two additional factors that may help explain why the population of nitrosobenzene adducts (as opposed to phenylnitrene adducts with subsurface oxygen) is so high following cyclocondensation. First, unlike cycloaddition reactions, cyclocondensation reactions produce a water molecule. The removal (desorption) of this molecule decreases the thermal energy available for further transformation of surface adducts. Second, also unlike cycloaddition reactions, cyclocondensation reactions are conducted in liquid nitrobenzene, which allows for thermal relaxation of the surface by energy exchange with the nearby molecules, also decreasing the thermal energy available for further transformation of surface species.

Finally, it can be noted that in the N *1s* XPS spectra collected following cyclocondensation processes for nitrobenzene both on hydrogen-terminated Si(100) and on hydrogen-terminated Si(111) surfaces, there is a noticeable, albeit small, peak observed at energy between 401 and 402 eV. This peak does exhibit the energy predicted for species D or G on hydrogen-terminated Si(100) and for species J on hydrogen-terminated Si(111); however, considering the energy diagrams described above, the presence of any of these species on a surface at room temperature is highly unlikely. The more plausible explanation of this observation is the reactions of nitrobenzene with various surface defects.

## V. Conclusions

A combination of IR, XPS, and theoretical investigations provide the proof of a cyclocondensation process on hydrogen-terminated Si(100) and Si(111) surfaces. The IR studies confirmed the loss of hydrogen from the surface and the attachment of the compound with the phenyl ring and C−N bond intact. The XPS data helped confirm the nature of the nitrogen-containing surface species. The theoretical calculations support both the XPS and the IR data. This provides a new method for ex situ attachment of organic molecules to hydrogen-terminated Si(100) and Si(111) substrates. Considering that this is a very simple and highly selective surface modification approach that can be easily controlled by thermal conditions, this reaction scheme will certainly find numerous applications for surface functionalization of semiconductor substrates.

**Acknowledgment.** The National Science Foundation (CHE-0415979) is acknowledged for the support of this research. The authors would like to thank Professor T. P. Beebe, Jr. and Mrs. M. E. Boggs for the XPS measurements made with NSF-supported instrumentation in the UD Surface Analysis Facility (DMR-9724307 and CHE-9814477). The authors would also like to acknowledge Professor Kate Queeney of the chemistry department of Smith College for her help with the detailed RCA cleaning procedure and subsequent etching procedures.

**Supporting Information Available:** Additional vibrational spectra and Cartesian coordinates of the key computational models considered, a list of uncorrected vibrational frequencies, and a complete ref 32. This material is available free of charge via the Internet at http://pubs.acs.org.

JA802645T